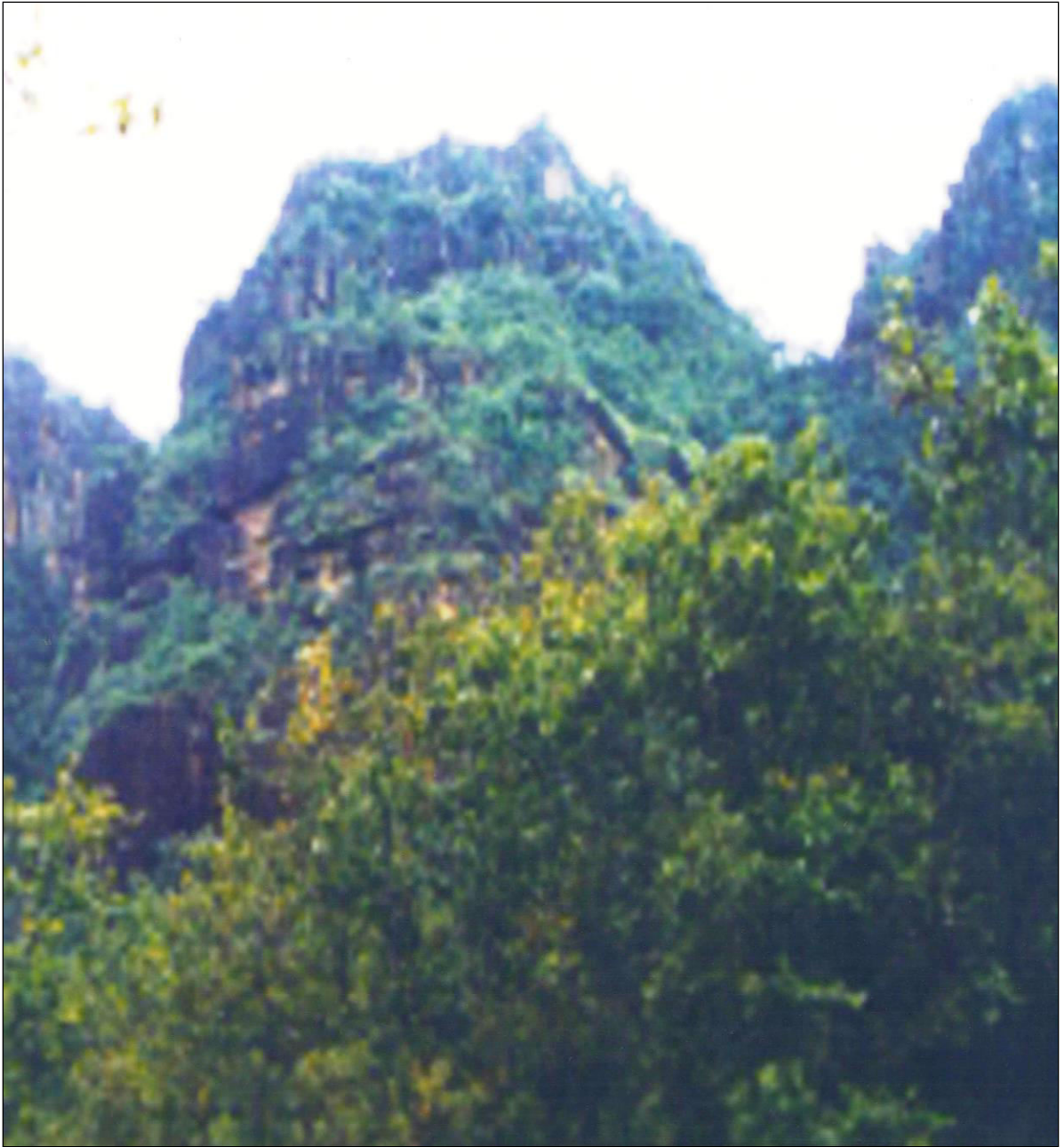


Folding Mechanism in the Pachmarhi

Dr. N.L. Dongre



ABSTRACT - This paper presents an introduction to the theory of folding of stratified viscoelastic media under compression and discusses its significance in the context of tectonics and orogenesis. Simplified derivations are given for results obtained earlier by the writer as particular cases of more elaborate theories. The writer emphasizes the mechanism involved in folding. The paper begins

with a discussion of the buckling of an elastic rod that is under axial compression and is restrained laterally by viscous dashpots. The analysis then proceeds to the analogous problem for an elastic and a viscous plate surrounded by a viscous medium. Results of some of the more complex problems previously analyzed by the writer are also applied and discussed. Experimental verification of the theory by model tests is presented in a companion paper (Biot, Ode, and Roever, 1961). A new feature of the present approach is the emphasis on rate phenomena and time histories in tectonic folding. In purely static problems of elastic buckling, a sharply defined wavelength is associated with the instability. By contrast, for viscoelastic media, the present theory leads to the concept of dominant wavelength and band width selectivity in analogy with the theory of electric wave filters. This is well illustrated by the gradual appearance of near-regular folds when a purely viscous layer surrounded by a viscous medium of lower viscosity is subjected to a compression in a direction tangent to the layer. The theory is applied to specific examples of geological interest. These include the case of a single layer or a superposition of layers. The case of a continuously inhomogeneous medium under similar forces is also included. Using accepted values of rock viscosity and elastic moduli, the writer finds that the time required for significant folding to take place agrees very well with the geological time scale. Folding may occur under tectonic stresses that are small in comparison with the crushing strength of the rock. The time history of folding depends, of course, on initial irregularities of the layers, but after sufficient time the folding becomes fairly insensitive to the magnitude and the distribution of the initial disturbances. The writer concludes that the viscous mechanism tends to predominate in tectonic folding. As a theoretical consequence, the wavelength of the folds will, in general, not be sensitive to the magnitude of the tectonic stresses unless gravity forces become important. The calculated wavelengths are in good agreement with the range of observed values. The point at which plastic or brittle failure occurs is found to depend primarily not on the magnitude of the strain but on deformation rates. The theory can be applied to materials with nonlinear stress-strain characteristics, and the procedure to accomplish this is briefly discussed. Certain nonlinear features resulting from the geometry of deformation are shown to have a bearing on the regularity of the folds.

Regional disturbance in the Mahadevas is a maximum along the edge of the Narbada valley, where the rocks are often crumpled into sharp folds. These rapidly die out in a southerly direction till, at their junction with the Bijoris, the Mahadevas lie almost horizontally. The Paehmarhi rocks, which are almost horizontal all along the southern scarp of the Mahadeva range, dip at about 10° to the north to form the northern slopes of those hills. They are further folded between Dhansai and the Tawa River into a well marked syncline with steep southerly dips along its northern edge. It is due to a gentle easterly pitch in this syncline that the main outcrop of Paehmarhi sandstone is rounded off in this vicinity. This synclinal fold has doubtless affected the underlying rocks which are here sandstones and red clays, but as these outcrop in a flat sandy plain where exposures are rare, the syncline could not be traced further to the west. In any event, it must be cut off sharp by an important fault which crosses this area near Dhansai. East of the

Tawa river, this syncline is lost beneath a tongue of Bagra conglomerate, which stretches south over the upturned edges of the Pachmarhis with marked unconformity. Further east the Pachmarhis reappear in the plain of Magaria. They form here an anticlinal fold cut off sharply to the north by a fault, and developing a steep easterly pitch in the country east of Police Station, Pachmarhi. Denwas, Bagras, and even Jabalpurs have been involved in this folding. To the south, this fold flattens gradually towards the Denwa river and ultimately becomes the northern limb of the great syncline in which the Denwa river flows between Khapa ($22^{\circ} 33' : 78^{\circ} 3'$) and the Piparia-Chhindwara main road. This folding dies out in the region lying east of this road, for there are very marked structural features in the Dudhi valley but only low dips varying rapidly from place to place.

In the present paper, the writer emphasizes the linear aspects of the folding theory through the Pachmarhi Mahadeva Model. However, the theory can easily be extended to apply to nonlinear materials in two ways. First, in the incipient phase of folding, the stress in the layer may be high enough to be in the range where the relationship between creep rate and stress is nonlinear. In this case, the theory will apply for incipient folding, provided that a viscosity coefficient that represents the linear dependence between stress increments and small creep-rate increments is used. This "effective viscosity coefficient" will be stress-dependent. The next phase will be characterized by the local appearance of plasticity, fracture, and high creep rates. The occurrence of this phase will generally be associated with large deformations, unless the initial compression itself is very high. The point at which these effects become significant can be evaluated by calculating the stresses on the basis of the linear theory. When localized yielding or fracture occurs, one can extend the calculation to this phase by applying the present linear theory, taking into account the local in-homogeneities, and by using the concept of "effective viscosity." In addition to the "physical" nonlinearities just mentioned, which originate in the physical nature of the materials, other nonlinear features are involved. They might be called geometrical, since they arise when deflections are "large." The result, for instance, is to shorten the distance between crests of the folds over the value given by the linear theory. Such corrections are easily introduced by elementary considerations. These points are discussed briefly at the end of Section 6. Other features arising from nonlinearity are of geometric origin and are due to the amplitude limitation of the folds. As explained at the end of section 5 this limitation tends to increase the regularity of the folds. Further development of the theory along this line is in progress and will be present theory.

2. Buckling of an elastic rod with viscous lateral restraint

To illustrate the qualitative aspect of the various problems treated hereafter, the writer discusses first a simple problem of instability. Let a thin rod be pinned at both ends A and B and be subjected to a total axial compressive load, F . Such a rod buckles under an axial compression given by the well-known Euler formula

$$F = \pi^2 \frac{EI}{a^2}, \quad (2.1)$$

Where E is Young's modulus of the elastic material, the movement of inertia of the rod's cross section, and $a = AB$, its length.

The deflection between points A and B is a half wave, and, within the limitations of a linear theory, equilibrium is maintained for an arbitrary amplitude of the deflection, *i.e.*, the equilibrium is neutral. Another way of stating this is by saying that under the axial compression (2.1), the rod deflects laterally by a finite. Instead of a rod of length a , let us consider a rod of

infinite length that is subject to the same compressive load, F . Let the rod be pinned at equidistant points A, B, C, D , etc. (Figure 1), the distance between the points being equal to a . Each section can then be assimilated to the pinned rod of length a , which we have just considered, and each of these sections will buckle in a half sine wave. This rod of indefinite length will then exhibit a sinusoidal deflection of wavelength

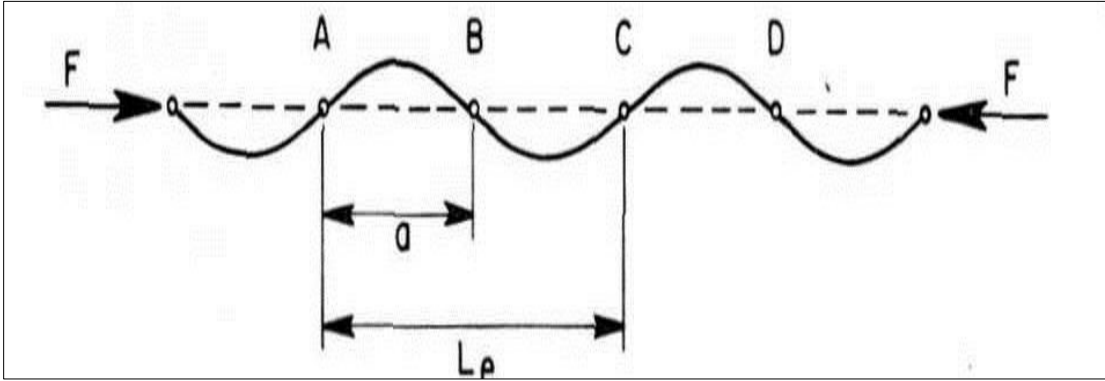


Figure 1. Instability of a thin rod under an axial compression F . The rod will buckle in many waves, provided it is restrained at the nodes A, B, C and D . amount under an infinitesimal lateral load.

We shall refer to this length as the Euler wavelength associated with the compressive load F . Note that the rod exerts no lateral force on the pins at points A, B, C, D , etc. The restraint is therefore introduced only to indicate how an experiment could actually be performed showing such a sinusoidal deflection. Without the pins, of course, the system would be unstable, and the rod would immediately collapse with the appearance of larger buckling wavelengths.

Let us now maintain a fixed compressive load, F , but vary the distance between pins, *i.e.*, vary the wavelength, L . For wavelengths smaller than the Euler wavelength, L_e the deflection cannot be maintained and will suddenly disappear. For wavelengths larger than let the deflection will increase and the rod will collapse, unless we introduce a lateral load to prevent this. To evaluate the magnitude of the lateral force required to do this, we shall use the familiar equations for the deflection of a beam in the theory of structures. We shall assume that the rod can deflect only in the plane of the figure. The x co-ordinate lies along the axis of the undeformed rod, and w denotes the deflection perpendicular to this direction. The bending moment, M is proportional to the curvature, d^2w/dx^2 , of the rod.

$$L_e = 2a, \quad (2.2)$$

This relationship is

$$EI \frac{d^2w}{dx^2} = -M \quad (2.3)$$

The sign conforms to the directions indicated in Figure 2 for positive bending moments. The bending moment is made up of two parts,

$$M = M_1 + M_2, \quad (2.4)$$

The term M_1 is the bending moment due to the axial load F_1 ;

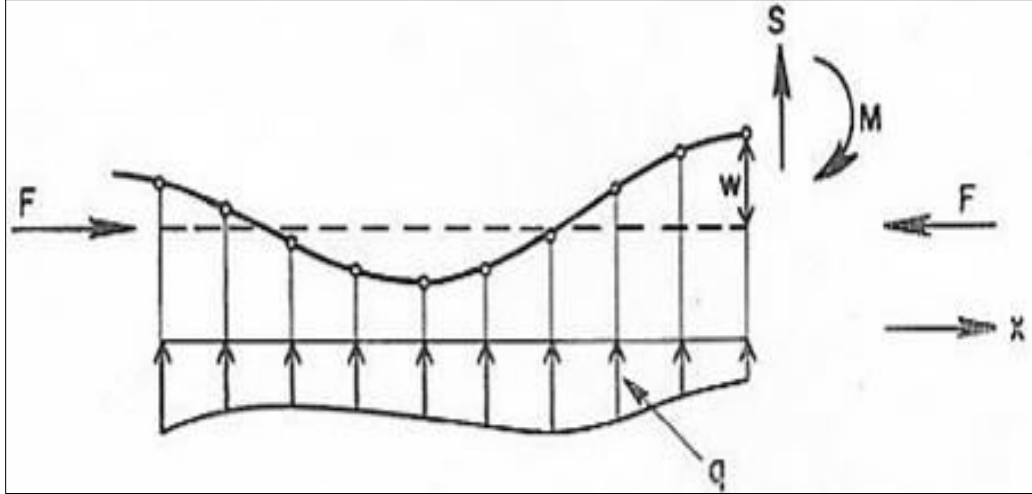


Figure 2 . Balance of forces in a rod that buckles under an axial compression F and is laterally restrained by viscous dashpots.

$$M_1 = Fw, \quad (2.5)$$

The term M_2 is the bending moment due to the lateral restraining forces. These forces are assumed to act perpendicularly to the rod axis. The magnitude of this force per unit length is designated by q , and the sign is chosen positive when q , is acting in the positive direction of the deflection ω . The following relationships can be written:

$$\frac{dS}{dx} = -q, \quad \frac{dM}{dx} = S, \quad (2.6)$$

where S represents the shearing force on the rod cross section due to q , and

$$\frac{d^2M}{dx^2} = -q, \quad (2.7)$$

Combining equations (2.3), (2.4), (2.5), and (2.7), we derive

$$q = F \frac{d^2w}{dx^2} + \frac{d^4w}{dx^4}, \quad (2.8)$$

The sinusoidal deflection of the rod is represented by

$$w = w^0 \cos lx, \quad (2.9)$$

where the wavelength of the deformation is

$$L = \frac{2\pi}{l}, \quad (2.10)$$

The transversal load necessary to maintain this deflection is also distributed sinusoidally *i. e.*,

$$q = q^0 \cos lx, \quad (2.11)$$

Relation (2.8) can therefore be written

$$-q = fl^2w - EIl^2\omega, \quad (2.12)$$

The quantity $-q$ represents the force with which the rod is pushing against the lateral constraint. It is represented by two terms. The first, fl^2w , is a driving force generated by the compression, F , and the curvature of the rod. The second term, $EIl^2\omega$, represents the restraint against deformation due to the bending rigidity. There is a wavelength for which these two terms are equal, i.e., for which $q = 0$. The value of l for which this occurs corresponds to the Euler wavelength

$$L_e = 2\pi\sqrt{\frac{EI}{F}}, \quad (2.13)$$

This corresponds to equation (2.1), if we put $2a = L_e$. For wavelengths larger than this value, the rod pushes against the lateral constraint, and it can be seen that there is a certain wavelength for which the magnitude of this push will be a maximum. Finally, we shall specify the nature of the lateral constraint. We shall assume that it is made up of a continuous distribution of viscous dashpots, such that the restraining force is proportional to the time derivative of the deflection, namely,

$$-q = b\frac{dw}{dt}, \quad (2.14)$$

Substituting in equation (2.12) yields

$$b\frac{dw}{dt} = w(Fl^2 - EIl^4), \quad (2.15)$$

This is a differential equation for w , and its general solution is

$$w = Ce^{pt}, \quad (2.16)$$

with

$$p = \frac{1}{b}(Fl^2 - EIl^4), \quad (2.17)$$

For wavelengths smaller than L_e , the value of p is negative, and the deflection will die out. Any sinusoidal deflection of wavelength larger than L_e is unstable, since p is then positive. Its amplitude increases exponentially. The value of l for which p is a maximum is

$$l_d = \sqrt{\frac{F}{2EI}}, \quad (2.18)$$

This corresponds to the wavelength for which the rate of increase of the amplitude is maximum. We shall call this the dominant wavelength L_d . Its value is

$$l_d = 2\pi\sqrt{\frac{2EI}{F}} = \sqrt{2}l_e, \quad (2.19)$$

The dominant wavelength is $\sqrt{2}$ times the Euler wavelength, is a function of the compressive load, and is independent of the viscosity of the lateral constraint.

The physical significance of this dominant wavelength lies in the fact that the initial deviations of the rod axis from a perfect straight line can be expanded in a Fourier series. Each

component is characterized by its own wavelength, and its amplitude will increase exponentially at a certain rate. The dominant wavelength will possess a much larger rate of deformation than others and is therefore the one most likely to be observed in practice. A certain amount of scatter of the observed wavelengths around the value L_e must be expected, owing to the randomness of the initial irregularities. The writer calls attention to the physical significance of the Euler wavelength, l_e , which acts as a cutoff wavelength. For all wavelengths smaller than l_e the value of ρ (equation 2.17) is negative. The Euler wavelength depends on the load, and if the load is suddenly decreased, all wavelengths which had appeared and are now smaller than the new value of L_e will gradually disappear.

In deriving these equations, we have neglected all inertia forces. This is justified, since we have in mind applications to viscous solids in which rates of deformation are very small. (Srivastava and Rastogi Year 2010)

3. Buckling of an elastic plate in a viscous medium

We consider now an elastic plate of thickness h embedded in an infinite viscous continuum. The geometry is illustrated in Figure 3. We choose the x axis parallel to the plate and the y axis perpendicular to it. The plate is infinitely extended. A uniform compression, P , per unit area is acting in the plate in the x direction. We are interested in the buckling of this plate and in the appearance of a sinusoidal deflection along x . The deformation is one of two-dimensional strain in the x, y , plane. In analyzing such a deformation, we may imagine that the plate is represented by a strip of unit thickness in the direction perpendicular to x, y . We can then treat the problem of buckling of this strip in a manner entirely analogous to that of the rod analyzed heretofore. There are, however, two essential differences.

The first difference arises from the fact that we are dealing with two-dimensional strain. The stress-strain relationships in the x, y plane are

$$\begin{aligned}\sigma_{xx} &= 2\mu e_{xx} + \lambda(e_{xx} + e_{yy}), \\ \sigma_{yy} &= 2\mu e_{yy} + \lambda(e_{xx} + e_{yy}),\end{aligned}\tag{3.1}$$

where λ and μ are Lamé coefficients. In the bending deformation of the plate, we can put

$$\sigma_{yy} = 0,\tag{3.2}$$

We derive,

$$\sigma_{xx} = B e_{xx},\tag{3.3}$$

with

$$B = \frac{4\mu(\mu+\lambda)}{2\mu+\lambda} = \frac{E}{1-\nu^2},\tag{3.4}$$

In this expression, E is Young's modulus and ν is Poisson's ratio for the plate. We see that for two-dimensional strain, Young's modulus must be replaced by B . On the other hand, the moment of inertia, I of the cross section is, in this case,

$$I = \frac{h^3}{12},\tag{3.5}$$

Equation (2.3) is therefore replaced by

$$\frac{1}{12} Bh^3 \frac{d^2 w}{dx^2} = -M, \quad (3.6)$$

The total compressive load which plays the role of F is

$$F = Ph, \quad (3.7)$$

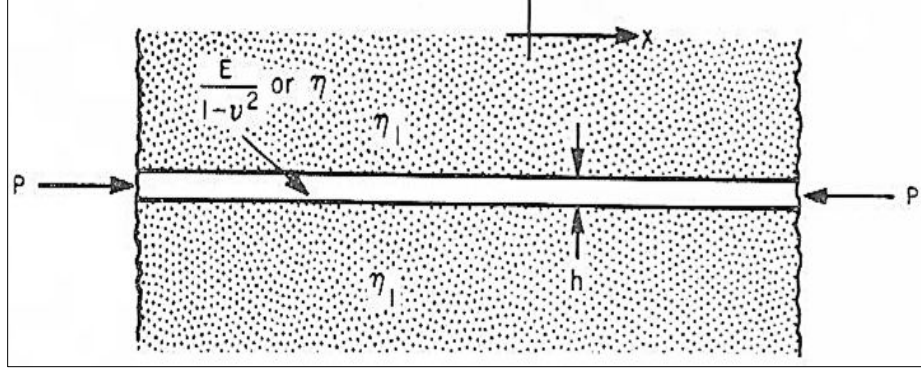


Figure 3 . Elastic plate of effective rigidity $E/(1 - \nu^2)$ (E , Young's modulus; ν^2 Poisson's ratio) or viscous layer of viscosity η embedded in a viscous medium of viscosity η_1

Equation (2.8) must, therefore, be replaced by

$$q = \frac{Ph}{12} \frac{d^2 w}{dx^2} + \frac{1}{12} Bh^3 \frac{d^4 w}{dx^4}. \quad (3.8)$$

This is the load, q per unit area required to maintain a deflection, w of the plate under the axial compression P . For a sinusoidal deflection (equation 2.9), we write

$$-q = phl^2 w - B \frac{h^3}{12} l^4 w, \quad (3.9)$$

The second difference from the problem in the previous section is that the lateral constraint is due to a viscous continuum instead of to local dampers. The load per unit area required to deflect a semi-infinite viscoelastic medium has been evaluated. (Craster and Millery, 2009) The result is expressed as follows.

The normal load, q per unit area acting at the surface is assumed to be distributed sinusoidally (Figure 4). We write

$$q' = q'_0 \cos lx, \quad (3.10)$$

The deflection, w , of the surface is also distributed sinusoidally. Its positive direction is chosen the same as that of q' . If the material is an incompressible viscous solid of viscosity η_1 , the relationship between load and deflection is

$$q' = 2\eta_1 l \frac{dw}{dt}, \quad (3.11)$$

The plate acts upon two such half-spaces, one on each side; therefore, we can write

$$-q = 2q' \quad (3.12)$$

$$-q = 4\eta_1 l \frac{dw}{dt}, \quad (3.13)$$

Comparing this with equation (2.14), we note an essential difference in the fact that the viscous-resistance factor $4\eta_1 l$ of an equivalent dashpot contains the quantity l . Hence, the viscous resistance of the medium per unit area is inversely proportional to the wavelength. This is essentially due to a similarity law for the half-space. In that respect, it is entirely analogous to the case of an elastic half-space. In the latter case, if the same specific load is distributed over similar areas of different dimensions, the deflection is proportional to the linear dimension of the area. Combining equations (3.9) and (3.13), we derive

$$4\eta_1 \frac{dw}{dt} = Phlw - \frac{1}{12} Bh^3 l^3 w, \quad (3.14)$$

The solution of this differential equation is again given by the general formula (2.16). The exponential rate of deformation is measured by the rate is zero for the value of l that cancels

$$p = \frac{1}{4\eta_1} \left(Phl - \frac{1}{12} Bh^3 l^3 \right), \quad (3.15)$$

the right-hand side, *i.e.*, for the Euler wavelength,

$$L_e = \pi h \sqrt{\frac{B}{3P}} = \pi h \sqrt{\frac{E}{3(1-\nu^2)P}}, \quad (3.16)$$

The value of p is a maximum for $l = l_d$, where

$$l_d h = 2 \sqrt{\frac{P}{B}}, \quad (3.17)$$

This yields the dominant wavelength

$$L_d = \pi h \sqrt{\frac{B}{P}} = \pi h \sqrt{\frac{E}{(1-\nu^2)P}}, \quad (3.18)$$

$$L_d = \sqrt{3} L_e,$$

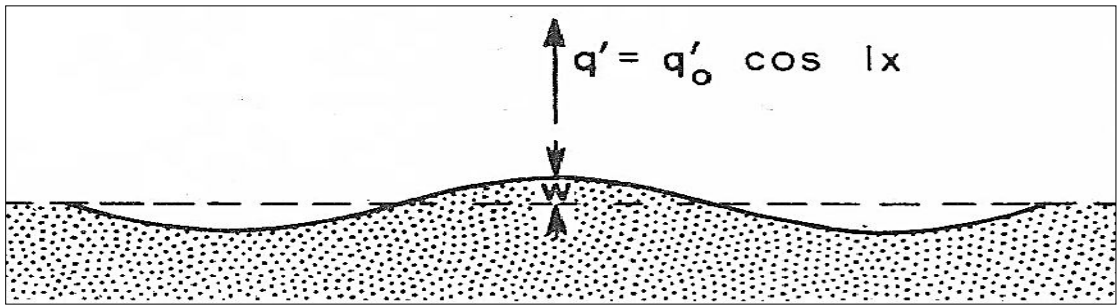


Figure 4. Deflection of the viscous embedding medium at the surface of contact with the layer and the restraining force q' , of the medium

In this case of a plate restrained by a viscous continuum, the ratio of L_d/L_d is $\sqrt{3}$, as compared to $\sqrt{2}$ for the rod restrained by dashpots. This is due to the dependence of the viscous resistance on the wavelength in expression

As mentioned in the previous section, the Euler wavelength, L_e , acts as a cutoff wavelength. Its value depends on the compressive load, and any wavelength component smaller than L_e present in the deformation at any particular instant will tend to disappear.

4. Folding instability of a compressed viscous plate in a viscous medium

We shall now consider the case in which the elastic plate of the previous problem is replaced by a layer of incompressible, purely viscous solid of viscosity coefficient η . The plate of thickness h (Figure 3) is subject to a longitudinal compression, P , per unit area. It is embedded in an incompressible; purely viscous, indefinite medium of considerably lower viscosity η_1 . We can visualize an experiment in which the plate and the medium are squeezed together at a uniform constant rate in a direction parallel with the plate. We are concerned here with the stability of this state of uniform deformation of the plate and the medium. In particular, we shall investigate the possibility of sinusoidal folding of the plate when a small perturbation is introduced in the system. Such a perturbation is, for instance, a deviation of the plate from a perfectly flat surface. By Fourier expansion of such deviation, this amounts to examining how a perturbation constituted by a single sinusoidal wave in the deflection of the plate will grow in amplitude as a function of time. (Tikoff, and Czeck, 2008) In analyzing this problem, we shall neglect the compressive stress, P_1 , in the surrounding medium. To analyze the deformation in this problem, we must consider the stress-strain relationships for an incompressible viscous medium in two-dimensional strain. The stress and strain in the plane are related by the equations

$$\sigma_{xx} - \sigma = 2\eta \frac{\partial e_{xx}}{\partial t}, \sigma_{yy} - \sigma = 2\eta \frac{\partial e_{yy}}{\partial t}, \quad (4.1)$$

where

$$\sigma = \frac{1}{2} (\sigma_{xx} + \sigma_{yy}), \quad (4.2)$$

The x axis is shown parallel with the plate. If free expansion is allowed in the y direction, *i.e.*, normal to the plate, we can put $\sigma_{yy} = 0$. Then

$$\sigma_{xx} = 4\eta \frac{\partial e_{xx}}{\partial t}, \quad (4.3)$$

Hence, a uniform rate of strain, de_{xx}/dt , will produce a constant compressive stress in the plate:

$$P = -4\eta \frac{\partial e_{xx}}{\partial t}, \quad (4.4)$$

The same rate of strain in the surrounding medium produces a compressive stress

$$P_1 = -4\eta_1 \frac{\partial e_{xx}}{\partial t}, \quad (4.5)$$

This is the initial steady state of the system upon which we shall now superpose a sinusoidal bending deformation of the plate.

The bending of a viscous plate can be treated in a manner entirely analogous to that of an elastic plate. The appearance of bending introduces a bending moment, M in the viscous plate proportional to the rate of change of its curvature. The following relationship is easily derived:

$$\frac{1}{3} \eta h^3 \frac{\partial^3 w}{\partial x^2 \partial t} = -M, \quad (4.6)$$

This equation is formally the same as relationship (3.6), provided that we introduce the formal identity

$$B = 4\eta \frac{\partial}{\partial t}, \quad (4.7)$$

Proceeding exactly as in the case of an elastic plate, we establish the analogue of expression (3.8) for the transversal load, q acting on the plate:

$$q = Ph \frac{\partial^2 w}{\partial x^2} + \frac{1}{3} \eta h^3 \frac{\partial^5 w}{\partial t \partial x^4}, \quad (4.8)$$

For a sinusoidal deformation, this becomes

$$-q = Phl^2 w - \frac{1}{3} \eta h^3 l^4 \frac{dw}{dt}, \quad (4.9)$$

The load, $-q$, is the reaction of the viscous medium to deformation. Its expression is given by equation (3.13). Hence, we derive

$$4\eta_1 l \frac{dw}{dt} = Phl^2 w - \frac{1}{3} \eta h^3 l^4 \frac{dw}{dt}, \quad (4.10)$$

This is a differential equation for the deflection w . As before, the solution for w is proportional to the exponential e^{pt} , and p is given by

$$p = \frac{P}{\frac{4\eta_1}{hl} + \frac{1}{3}\eta h^2 l^2}, \quad (4.11)$$

This expression depends on the wavelength through the non-dimensional variable lh . For zero and infinite wavelength, *i e.*, for $l = \infty$ and $l = 0$ the value of p is zero and the rate of deformation of any sinusoidal bending is zero. For an intermediate value of l the value of p goes through a maximum. The value of l at which this happens is given by $l = l_d$, where

$$l_d h = \sqrt[3]{\frac{6\eta_1}{\eta}}, \quad (4.12)$$

The corresponding dominant wavelength is

$$L_d = 2\pi h \sqrt[3]{\frac{\eta}{6\eta_1}}, \quad (4.13)$$

The ratio of dominant wavelength to thickness, L_d/h is shown in Table 3 as a function of the viscosity ratio, η/η_1 . The value $p = p_m$ the dominant wavelength is found by putting $l = l_d$ in expression (4.11). We find

$$p_m = \frac{p}{6\eta_1} \sqrt[3]{\frac{6\eta_1}{\eta}}, \quad (4.14)$$

This expression determines the rate of growth of the amplitude of folding at the dominant wavelength.

We note the important fact that for a viscous plate in a viscous medium, the *dominant wavelength is independent of the compressive load, P*. This is in contrast with the case of the elastic plate. The load, of course, affects the rate of deformation, but, as shown by relation (4.11), all wavelengths are equally affected.

The case of the viscous plate also differs from that of the elastic plate by the absence of a cutoff wavelength, *ie.*, all wavelengths are amplified.

5. Amplification and selectivity of folding

The writer must call attention to certain important features of folding, which are characterized by two aspects. One is the degree of amplification, *ie.*, the magnitude of the factor by which a certain wavelength amplitude initially present in the layer is multiplied after a given time. Another is the selectivity of the amplification. This can be characterized by the band width representing those wavelengths that are selectively amplified. These concepts are entirely analogous to those encountered in the theory of electronic wave filters.(Ferrill and morris, 2008)

Let us first consider the case of an elastic layer in a viscous medium. The amplification factor, after an interval of time, is

$$A = e^{pt}, \quad (5.1)$$

where p is a function of the wavelength given by equation (3.15). The maximum value, A_d , of this amplification occurs for the dominant wavelength, $i, e,$ for $i = l_d$ We write

$$A_d = e^{Pm^t}, \quad (5.2)$$

where p_m is the maximum value of $p, i. e;$

$$p_m = \frac{1}{6} l_d h \frac{P}{\eta_1} = \frac{1}{3} \frac{P}{\eta_1} \sqrt{\frac{P}{B}}, \quad (5.3)$$

We can plot the amplification at any given time as a function of the wavelength or, more conveniently, as a function of the wave number, l (Figure 5).

There are two wave numbers, l_1 and l_2 , for which the amplification is one-half the maximum value, *ie.*, for which

$$A = \frac{1}{2} A_d, \quad (5.4)$$

This is an equation for l_1 and l_2 which is equivalent to

$$1 - \frac{p}{p_m} = \frac{\log 2}{p_m t} = \frac{\log 2}{\log A_d}, \quad (5.5)$$

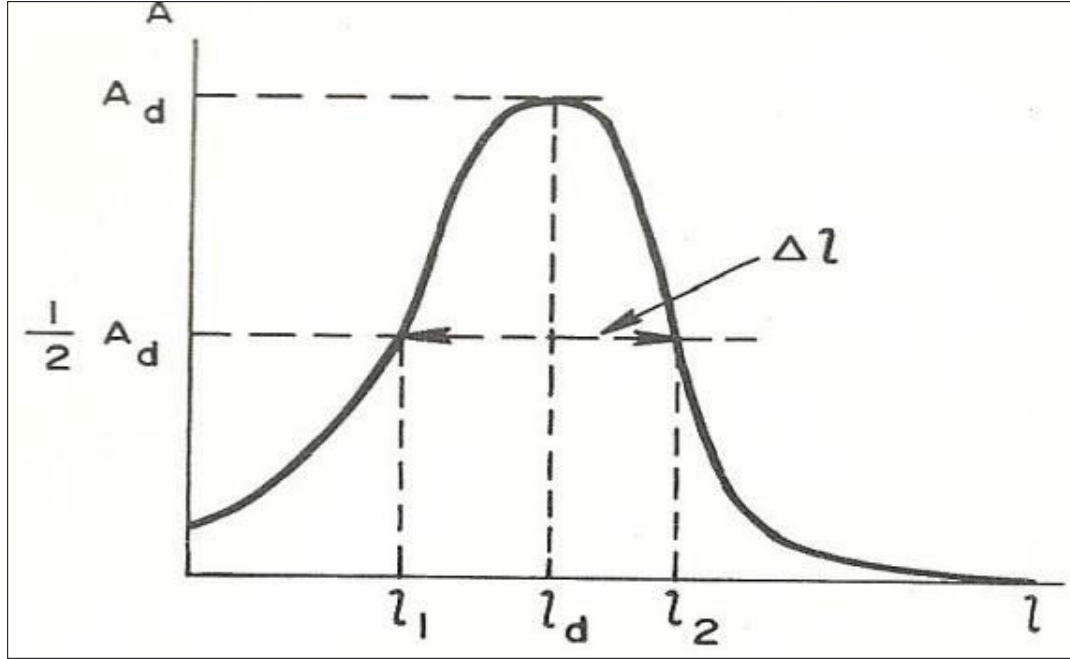


Figure 5 . Amplification, A , of the folding as a function of the wave number

(\log denotes the natural logarithm.)

The selectivity is determined by the relative band width

$$\frac{\Delta l}{l_d} = \frac{l_2 - l_1}{l_d}, \quad (5.6)$$

Equation (5.5) can be solved approximately by expanding the left-hand side in the vicinity of its minimum and retaining only the term that corresponds to the osculating parabola. We find

$$\frac{\Delta l}{l_d} = 2 \sqrt{\frac{2 \log 2}{3 p m t}} = \frac{1.36}{\sqrt{\log A_d}}, \quad (5.7)$$

There are two immediate conclusions. The band width decreases as $1/\sqrt{t}$ and depends only on the amplification, A_d , of the dominant wavelength.

For decreasing values of $\Delta l/l_d$, the selectivity increases, and the folding more closely approaches a pure sine wave. The significance of the band width is illustrated by the fact that two waves of wave numbers $l_d + 1/2 \Delta l$ and $l_d - 1/2 \Delta l$ will, by superposition, produce amplitude beats. The interval between the beats is denoted by D , and we can write

$$\frac{L_d}{D} = \frac{\Delta l}{l_d}, \quad (5.8)$$

Table 1 shows the band width for various amplifications.

Table 1 . Band Width $(\Delta l/l_d)_e$ For the Elastic Layer in a Viscous Medium as a Function of the Amplification Factor A_d

A_d	$(\Delta l/l_d)_e$
-------	--------------------

(10	0.896
10 ²	0.635
10 ³	0.516
10 ⁴	0.448
10 ⁵	0.400

As can be seen, the selectivity varies slowly with the amplification. A Certain regularity in the waves will begin to appear at amplifications of 10². Theoretically, of course, the amplification may grow to infinity. Since the amplitude of the folding remains finite, this can be the case only when the folding is initiated in a layer in which initial imperfections are smaller and smaller. The closer we come to an initially perfectly flat layer, the smaller (Cosgrove, 2007) will be the band width, and the more regular will be the appearance of the folding.

Let us now turn to the case of a viscous layer in a viscous medium. According to (4.14), the maximum value p is

$$p_m = \frac{P}{6\eta_1} \sqrt[3]{\frac{6\eta_1}{\eta}} = \frac{p}{\eta} \left[\frac{\eta}{6\eta_1} \right]^{2/3}, \quad (5.9)$$

We can represent the selectivity by a band width, as above. We write an equation identical to (5.5), except that p_m is given by (5.9) and p by (4.11). Proceeding as above, and using the same type of approximate solution of equation (5.5) to determine the band width, we find

$$\frac{\Delta l}{l_d} = 2 \sqrt{\frac{\log 2}{pmt}} = \frac{1.66}{\sqrt{\log A_d}}, \quad (5.10)$$

This expression differs only by a constant factor for the similar formula (5.7) for the elastic layer. The band width for the viscous layer at various amplifications, as given by (5.10), is shown in Table 2.

Table 2. Band width $(\Delta l/l_d)v$ for the Viscous Layer in the Viscous Medium as a Function of the Amplification Factor A_d .

A_d	$(\Delta l/l_d)v$
10	1.095
10 ²	0.775
10 ³	0.632
10 ⁴	0.548
10 ⁵	0.490

Comparing Table 2 with expression (5.7) and with Table 1 for the selectivity of the elastic layer, we note that the viscous layer has a larger band width. For the elastic layer, Table 1 indicates that a band width $\Delta l/l_d = 0.635$ is attained for an amplification of $A_d = 100$. Table 2 shows that for the same band width to be obtained in the case of the viscous layer, we must reach an amplification about 10 times larger. As a consequence, the elastic layer will tend to fold more regularly—a result that has been confirmed by model tests.

There is another interesting aspect by which the viscous layer differs from the elastic layer (Camerlo and Benson, 2006). For the elastic layer, by starting with layers that contain less

and less initial distortion from the ideal plane surface, we can attain arbitrarily larger amplification factors, provided we wait long enough. This is not so for the viscous layer, since the compressive load, P , produces a shortening of the layer that at a constant rate. If a significant amplification requires too long a time, the shortening of the layer will become so large that the folding phenomenon will be completely masked.

This can be brought out very clearly by a consideration of the time required for a given amplification to be obtained. This time is given by

$$t = \frac{1}{p_m} \log A_d, \quad (5.11)$$

when the value for p_m given in equation (5.9) is introduced, the time becomes

$$t = \frac{\eta}{1} \left[\frac{6\eta_1}{\eta} \right]^{2/3} \log A_d, \quad (5.12)$$

The quantity η / p is a time that has the following physical interpretation. Under the load P , the uniform compressive strain rate is given by equation (4.4), and the total compressive strain after a time t is

$$-e_{xx} = \frac{p}{4\eta} t, \quad (5.13)$$

when the compressive strain corresponds to a shortening of 25 per cent, the time elapsed is

$$t_1 = \frac{\eta}{p}, \quad (5.14)$$

with the reference time t_1 , expression (5.12) becomes

$$\frac{t}{t_1} = \left[\frac{6\eta_1}{\eta} \right]^{2/3} \log A_d, \quad (5.15)$$

It is of interest to show the dependence of the amplification factor, A_d on the viscosity ratio and the time ratio. This is shown in Table 3 for three values of the time, *i.e.*, $t = t_1/6$, $t = t_1/3$ and $t = t_1$.

These three values of t correspond to a shortening of the layer of 4.2, 8.8 and 25 per cent, respectively.

One important feature is immediately apparent from Table 3. Beyond a certain amplification, the amplitude of folding will increase at an explosive rate. This happens when $A_d \cong 1000$, and we can adopt this value as a standard. The time required for explosive amplification to occur is then given by relating (5.15) after $A_d = 1000$ is substituted. We find

$$\frac{t}{t_1} = 6.90 \left[\frac{6\eta_1}{\eta} \right]^{2/3}, \quad (5.16)$$

This time ratio for explosive amplification is a function only of the viscosity ratio.

As indicated in the discussion of band width, good selectivity also begins to appear for amplifications of about 1000; hence, sharp definition of the wavelength is also to be expected at these amplifications.

Another important feature brought out by Table 3 is the small amplification exhibited for viscosity ratios (η/η_1) smaller than 100.

Larger amplifications would, of course, appear for times t larger than t_1 . However, this would imply a shortening of the layer larger than 25 per cent. Such a large compressive strain would then overshadow the folding itself. We can conclude, therefore, that a clearcut folding with sharp definition requires that the viscosity of the layer be at least 100 times that of the medium. (Simpson, 2006)

Finally, at large viscosity ratios, the wavelength definition becomes very sharp. For instance, for $\eta/\eta_1 = 2000$, the amplification at the instant $t = t_3/3$ is of the order $A_d = 10^7$.

Table 3. Amplifications of the Amplitude of Folding at Times $t = t_1/6, t = t_1/3$ and $t = t_1$, as a Function of the Viscosity Ratio η/η_1 and Corresponding Ratios of the Dominant Wavelength L_d To the layer thickness, h .

$\frac{\eta}{\eta_1}$	$\frac{L_d}{h}$	$A_d t = \frac{t_1}{6}$	$A_d t = \frac{t_1}{3}$	$A_d t = t_1$
12	7.9	1.30	1.70	4.9
36	11.4	1.73	3.01	27.1
72	14.4	2.39	5.74	1.89×10^2
100	16.0	2.97	8.80	6.8×10^2
144	18.1	4.01	16.0	4.1×10^3
288	22.9	9.04	81.7	5.4×10^5
500	27.4	24.0	5.7×10^2	1.9×10^8
1,000	34.5	1.5×10^2	2.4×10^4	1.4×10^{13}
2,000	43.5	3.0×10^3	9.1×10^6	7.5×10^{20}
10,000	74.5	1.5×10^{10}	2.2×10^{20}	1.1×10^{61}

Substituting this value of A_d in expression (5.10) for the band width, we find

$$\Delta l/l = 0.415, \quad (5.17)$$

Using this value in equation (5.8) indicates that regular folds will appear over a distance D equal to about 2 1/2 times the wavelength. Of course, such large amplification can be achieved only for a layer whose initial deviation from a perfect plane is of the order of 10^7 of the wavelength.

The previous considerations on selectivity are applicable only within the range of validity of the linear theory. Attention should be called to a type of nonlinearity of geometric origin whose effect is to increase the regularity of the folds. This can be seen by considering a case of folding with uneven amplitude of the folds. Since the amplitude is limited by the geometry, the folds of greater amplitude will reach their limit first, while those of smaller amplitude will continue to grow. This will result in smoothing out of the uneven amplitudes and corresponds to an increase in selectivity. Here again we find an analogy in electronics. The phenomenon is not unlike the increase of selectivity obtained in the FM receivers by the use of amplitude limitation.

6. Geological aspects of the folding theory

We shall briefly discuss some of the previous results in the context of tectonics. Let us first consider the case of a viscous layer embedded in a viscous medium. It is reasonable to

assume that for very low stresses acting over long periods of time, the behavior of most rock is in the nature of a viscous medium. The analysis of Section 4, which neglects gravity, indicates that the existence of a very small compressive stress in the layer will immediately initiate folding. The wavelength of the folding will be characterized entirely by the ratio of the viscosity coefficients of the layer and of the medium and will be independent of the compressive load, P .

Viscosity coefficients of rock range widely. Accepted magnitudes of viscosity (Passchier ,Zhang and Konopasek, 2005) (Scanlin and Engelder ,2003) range from 10^{17} to 10^{22} poises. The figure 10^{17} is the order of magnitude of the viscosity for halite. These values correspond to pressures and temperatures near the surface of the earth. Some materials have lower values of viscosity. Viscosities will also be lower at higher pressure and temperature. The earth is, therefore, a highly heterogeneous medium from the standpoint of its flow properties. This is in contrast with the elastic properties, since the elastic moduli of rock generally range from 10^{11} to 10^{12} dynes/cm². It is clear, therefore, that folding in the earth must primarily reflect the large differences in viscous or viscoelastic properties.(Robin ,Allemand, Burov, Doin , Guillocheau, Dromart and Garcia, 2003)

As an example, let us consider a layer of viscosity $\eta = 10^{21}$ poises (*dynes cm⁻² sec⁻¹*) embedded in a medium of viscosity $\eta = 10^{18}$ poises. Let us assume also that the compressive load is $P = 10^8$ dynes/cm². This is about 1450 psi, *i.e.*, of the order of a fraction of the compressive strength of hard rock. The time required for the layer to shorten by 25 per cent is

$$t_1 = \frac{\eta}{P} 10^{13} \text{Sec} = 317,000 \text{ years}, \quad (6.1)$$

The dominant wavelength (*See* Table 3) is

$$L_d = 34.5 h, \quad (6.2)$$

where h is the layer thickness. The time, t , required for explosive folding to begin is given by equation (5.16); we find

$$\frac{t}{t_1} = 0.218, \quad (6.3)$$

Hence,

$$t = 72000 \text{ year} \quad (6.4)$$

At this time, the shortening of the layer is $t/4t_1$ or 5 percent.

Let us keep the same ratio of the viscosities $\eta / \eta_1 = 1000$, and consider other values for the viscosities and the compressive load, P . Table 4 shows the time required to reach explosive folding.

The time is shown in years, the load in pounds per square inch, and the viscosity in poise (cgs) units. These results fit in very well with the geological time scale.

If the viscosity ratio is $\eta/\eta_1= 100$, a similar table could be constructed in which the viscosities would be replaced by

$$\eta = 10^{22}, 10^{21}, 10^{20} \text{ cgs},$$

$$\eta_1 = 10^{20}, 10^{19}, 10^{18} \text{ cgs.} \quad (6.5)$$

When the same values for the compressive load are used, the time intervals are simply multiplied by the factor 4.65. The dominant wavelength in this case is

$$L_d = 16 h, \quad (6.6)$$

It can be seen that for periods of the order of 10^5 or 10^6 years, a *relatively small load may produce explosive folding, even in hard rock*. The wavelengths predicted are also within the range of observed values.

Table 4. Time in Years Required for Explosive Folding for a Viscous Layer in a Viscous Medium for Various Compressive Loads, P, and Viscosities

$\frac{P}{psi}$	$\frac{\eta}{\eta_1} \frac{10^{22}}{10^{19}}$ Year	$\frac{10^{21}}{10^{18}}$ Year	$\frac{10^{20} cgd}{10^{27} cgs}$ Year
14.5	7.2×10^7	7.2	
		$\times 10^7$	720,000
145.0	7.2×10^6	720,000	72,000
1,450.0	720,000	72,000	7,200
14,500.0	72,000	7,200	720

Our next step is to introduce the influence of the elasticity of the layer. We shall therefore examine the magnitude of the folding of a purely elastic layer in a viscous medium. The amplification factor, A_d , is related to the time by equations (5.2) and (5.3). They can be combined to read

$$t = t_e \log A_d, \quad (6.7)$$

With a characteristic time

$$t_e = \frac{3\eta_1}{p} \sqrt{\frac{B}{P}}, \quad (6.8)$$

The modulus B of the layer is denned by expression (3.4) and is close to Young's modulus of the material. The elastic module of rocks is in the range 10^{11} to $10^{12} \text{ dynes/cm}^2$, the latter value being close to the modulus of quartz. For the purpose of comparison, we shall adopt the highest value, $B = 10^{12} \text{ dynes/cm}^2$. Since t is proportional to \sqrt{B} , the variations of B within the allowable range for rock do not affect the order of magnitude of t . The viscosity, η_1 of the surrounding medium is assumed, as it was previously to lie in the range $\eta_1 = 10^{17}$ to $\eta_1 = 10^{20}$ poises. In analogy with our treatment of the viscous layer and also by examination of equations (5.2) and (5.3), it can be seen that explosive folding will start for the same value, $Ad = 1000$, for the amplification factor. Hence, the time at which explosive folding appears is given by

$$t = 6.90 t_e = 20.7 \frac{\eta_1}{p} \sqrt{\frac{B}{P}}, \quad (6.9)$$

This time is shown in years in Table 5, with $B = 10^{12} \text{ dynes/cm}^2$, for different values of the viscosity, η_1 , of the surrounding medium and of the compression, P , in the layer.

Table 5. Time in Years Required for Explosive Folding of an Elastic Layer in a Viscous Medium for Various Compressive Loads, P, in the Layer and Viscosities, η_1 , of the Medium Elastic modulus of the layer is $B = 10^{12}$.

P psi	η_1 cgs 10^{20}	10^{19}	10^{18}	10^{17}
	Year	Year	Year	Year
14.5	6.5×10^{10}	6.5×10^9	6.5×10^9	6.5×10^7
145.0	2.0×10^9	2.0×10^8	2.0×10^8	2.0×10^6
1,450.0	6.5×10^7	6.5×10^6	650,000	65,000
14,500	2.0×10^6	200,000	20,000	2,000

Comparison of these time intervals with those of Table 4 shows that much more time is required for the layer to fold as an elastic layer. This is particularly true for the smaller values of the compression, where the viscous phenomenon clearly predominates. At high values of the compression, of the order of 14,000 *psi*, the elastic property begins to influence the folding. We must remember, however, that such high loads are near the crushing strength, where plastic deformation and rupture will be introduced and will be superposed to the purely elastic deformation. Actually, of course, the rock will possess combined elastic and viscous properties, *i.e.*, it will be *viscoelastic*. It will tend to deform as a viscous solid at low rates of deformation, and, as this rate increases, the elasticity property will gradually enter into play. Calculation of the rate of folding for the more complex case of a viscoelastic layer can be carried out by applying the more elaborate theory (Biot, 1957) (Hickey And Bell , 2001) These considerations lead to the conclusion that the viscosity of the layer will, in general, tend to predominate over its elasticity.

On the other hand, at high loads the viscoelastic properties will tend to be masked by rupture and plastic deformation, particularly in regions of maximum bending. In this connection, we should also evaluate the bending stresses in the layer during the process of folding. The maximum stress will occur at the point of maximum amplitude, which is also the point of maximum curvature. Consider the folding of a viscous layer. The bending moment is given by equation (4.6). A sinusoidal deflection at the dominant wavelength is

$$w = w_t \cos l_d x, \quad (6.10)$$

where

$$w_t = w_0 e^{p m t}, \quad (6.11)$$

is the maximum amplitude at $x = 0$. The values of l_d and p_m are given by expressions (4.12) and (4.14). Using these values and substituting w in equation (4.6) for the bending moment, we find

$$M = \frac{1}{3} h w_t P, \quad (6.12)$$

By a well-known formula of plate theory, the maximum bending stress is

$$\sigma_m = \frac{6M}{h^2}, \quad (6.13)$$

Hence,

$$\sigma_m = \frac{2w_t}{h} P, \quad (6.14)$$

This stress is traction on the stretched side of the layer and a compression on the other. The stress must be superposed, of course, to the original compression in the layer. On the compressed side, the stresses due to bending and the initial compression are added, and the total compression is

$$\sigma_c = p \left[\frac{2w_t}{h} + 1 \right], \quad (6.15)$$

On the stretched side, the stresses are subtracted, and we obtain a tensile stress

$$\sigma_t = p \left[\frac{2w_t}{h} - 1 \right], \quad (6.16)$$

In the actual geological case, these stresses must also be superposed on the over-all hydrostatic pressure prevailing at the depth of the layer. (Burg and Podladchikov, 2000)

To illustrate the significance of this formula, let us consider the case of a layer of viscosity $\eta = 10^{21}$ poises embedded in a medium of viscosity $\eta = 10^{18}$ poises. For a layer 2 feet thick, the dominant wavelength will be 70 feet. Assume also a compressive load of 1450 psi in the layer and an initial deviation of the layer from a plane surface of the order of 0.1 inch over a distance of a wavelength, i.e., over a distance of 70 feet. From Table 4, we see that the time required for the layer to reach the state of explosive folding is of the order of 70,000 years. At that moment, the amplification factor is 1000, and the amplitude of the folds will be 100 inches. The folds will have the aspect shown in Figure 6a.

Consider the stress at a point of maximum amplitude, as given by equation (6.16). Substituting the values $P = 1450$ psi, $h = 24$ inches, and $w_t = 100$ inches, we find

$$\sigma_t = 10,600 \text{ psi}. \quad (6.17)$$

At such stress, cracks are likely to appear or some form of plastic deformation will occur, with a considerable increase in the creep rate equivalent to a decrease of the "effective" coefficient of viscosity as the stress increases. The stress at which this will occur depends not only on the nature of the rock but also on the hydrostatic pressure and temperature. In any case, a weakening of the layer is to be expected at points A and B of maximum amplitude. Further deformation will progress as though the layer were hinged at these points, producing a sharpening of the bends, as indicated in Figure 6b.

At the lower stress shown in Table 4, e.g., 145 psi, considerably more folding will have to occur before this type of failure will develop. On the other hand, at the higher stress, e.g., 14,500 psi, plasticity and fracture will occur almost immediately. At such high stresses, a theory based on elastic or viscous deformation can still be applied as an approximation if we assume that plastic deformations for incremental stresses obey relationships that on the average can be represented by an "incremental elastic modulus" or an "incremental coefficient of viscosity." In technological problems, a theory of buckling that makes use of the so-called "tangent modulus" has been successfully applied. Similarly, we could use the theories for either the viscous or the elastic layer, as developed above, provided that we substitute the appropriate coefficient representing average incremental properties. (Stipska, Schulmann, and Hock, 1999)

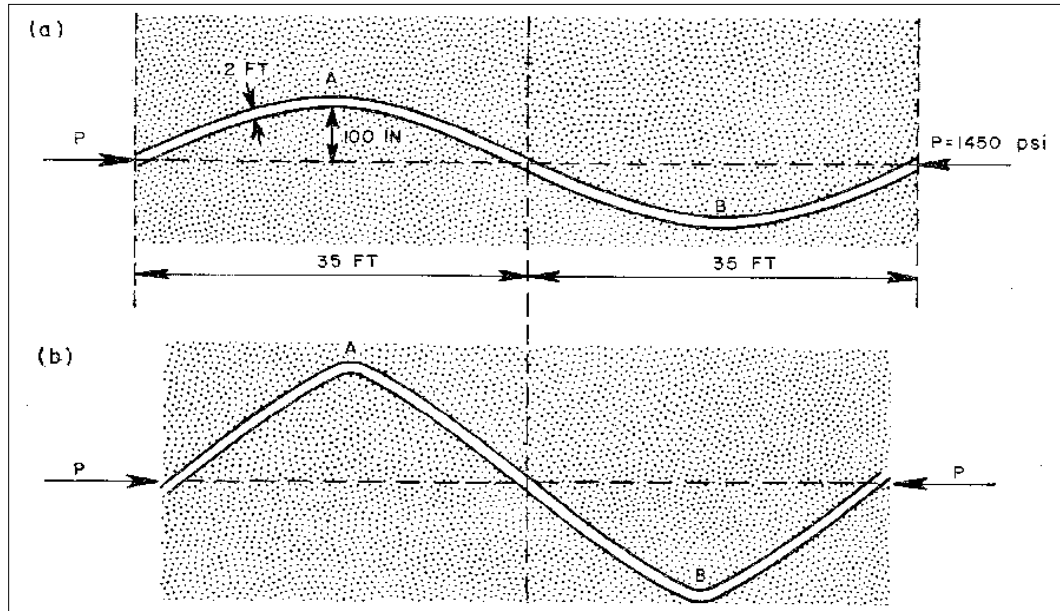


Figure 6 . folding of a layer 2 feet thick before and after yielding at the bends, (a) layer with a viscosity of $\eta = 10^{21}$ poises in a medium of viscosity $\eta = 10^{18}$ poises under a compressive stress $P = 1450$ psi. The amplitude is shown after 70,000 years. The assumed initial amplitude is one-tenth of an inch, (b) further deformation produces a sharpening of the folds due to yielding of the material at the bends.

The weakening of the layer at the point of maximum curvature would then be represented by a decrease in the effective elastic modulus or the effective viscosity coefficient as the stress increases. The significance of an effective viscosity is illustrated by considering a material whose rate of compressive deformation, $-\dot{e}$, is a certain function of the compressive stress, P . We can write this relationship as

$$-\dot{e} = f(P), \quad (6.18)$$

where $f(P)$ represents an empirical function. In the vicinity of a stress, P_0 , a small variation, dP , of the stress will produce a corresponding variation, $-d\dot{e}$, of the strain rate. The effective viscosity coefficient, η , is then defined by

$$\frac{1}{4\eta} = -\frac{de}{dP} = \frac{df(P_0)}{dP}, \quad (6.19)$$

The right-hand side represents the slope of the function $f(P)$ at the stress P_0 . In order to make the equation conform with the assumptions of the plate-bending theory, the strain, e , is taken as that of a plate whose deformation is free in the direction of the compression and in the direction normal to its plane but is restrained in its plane in the direction normal to the stress.

At this point, we must consider the significance of the characteristic time, t_1 if the material is nonlinear. In this case, t_1 , as defined by equation (6.1), does not represent the time in which an over-all shortening of 25 per cent of the layer takes place, since η represents the viscosity for incremental stresses. Actually, the time required for a 25 per cent shortening will be longer than t_1 by a factor $(df/dP) \times (P/f)$. This means that appreciable folding may occur for

effective viscosity ratios smaller than 100. Hence, when nonlinearity is introduced, significant folding may still occur for dominant wavelengths which are smaller than about 15 times the thickness.

By contrast, other nonlinear effects that are introduced here will primarily depend on the geometry or kinematics of the deformation for large displacements. Such (Butler, Spencer, and Griffiths, 1998) an effect will, for instance, be a shortening of the distance between crests of the folding. This will appear if the slope of the folding becomes appreciable. We have taken this into account in Figure 6 b.

An additional shortening of the distance between crests is a consequence of the shortening of the layer itself due to the constant action of the compressive stress. This shortening is proportional to t/t_1 , as defined previously. We have neglected this effect in our discussion, and it should be introduced as a correction depending on the magnitude of t/t_1 . For nonlinear materials, t_1 should be corrected according to our remark in the preceding paragraph.

It is of considerable interest to note that the stress in a viscous layer depends not on the magnitude of the strain but on its rate. (Burg nad Ford, 1997) This means that considerable bending can occur under a low compressive stress, P , without the appearance of cracks or plastic yielding.

Before concluding this section, we should also mention the magnitude of the dominant wavelength for the case of an elastic layer. Applying formula (3.18), assuming $B = 10^{11}$ dynes/cm² and $P = 14,500$ psi, we find

$$L_d \cong 30h, \tag{6.20}$$

We have assumed a compressive stress near the crushing strength; hence, the wavelength due to elastic bending of the layer will, in general, be larger than that given in equation (6.20). On the other hand, the observed wavelengths are usually smaller and tend to be closer to the values predicted from the assumption of purely viscous bending. This further confirms the conclusion that the viscous mechanism of folding tends to predominate.

7. Folding of multiple layers

We shall now consider the important case of a multiplicity of superposed layers that are separated by softer materials at their interfaces (Figure Id). To acquire an insight into the nature of this problem, let us first analyse the case of n superposed layers of equal thickness, h , and viscosity, η , assuming that perfect lubrication exists between the layers. This stack of layers is embedded in a medium of viscosity η_1 and is subject to a horizontal compression, P , per unit area.

This case is readily analysed by making use of the previous results for a single layer. All transversal forces acting on each layer must add up, so that if q is the transversal load with which the surrounding medium reacts on the whole stack, the load on each layer is q/n . Hence, the deflection, w , must satisfy the same equation (4.9) as for the single plate, q/n except that q must now be replaced by q/n . This is also equivalent to replacing η_1 by η_1/n in all equations obtained above for the single viscous layer in a viscous medium. The dominant wavelength (4.13) becomes

$$L_d = 2\pi h^3 \sqrt{\frac{n\eta}{6\eta_1}}, \quad (7.1)$$

A stack of $n = 10$ layers will show a dominant wavelength equal to $\sqrt[3]{10} = 2.16$ times the wavelength for a single layer.

All conclusions for a single layer are applicable to multiple layers, provided we change the viscosity ratio accordingly. (Hutton, 1982) For instance, in the numerical example just considered, assume a layer of thickness $h = 2$ feet and viscosity $\eta = 10^{21}$. We superpose 10 such layers, for a total thickness of 20 feet, and assume that they are embedded in a medium of viscosity $\eta_1 = 10^{18}$. The single layer then behaves as though it were embedded in a medium of viscosity 10 times smaller, *i.e.*, it behaves as the single layer with a viscosity ratio $\eta/\eta_1 = 10,000$. Using this ratio, we find that the length of time required for explosive folding, given by equation (5.16), is 15,500 *years*. The value of t_1 is the same as that given by equation (6.1). The dominant wavelength will be 150 feet. If we assume initial deviations of about one-quarter of an inch from the perfect plane over a distance of one wavelength, the aspect of the folding after 15,000 *years* will resemble that shown in Figure 7b.

The conclusions drawn for the single layer regarding further development of the folding beyond the linear range are applicable. We can use equations (6.15) and (6.16) to calculate the bending stresses. These stresses depend only on the compressive load, P , and the maximum deflection, ω_t . After 15,000 *years*, this deflection is about 11 feet. From equation (6.16), we derive the existence of a bending stress at that time of the order of

$$\sigma_t = 14,000 \text{ psi}, \quad (7.2)$$

At such a stress, cracks or plastic flow will begin to appear, along with a sharpening of the folds at the bend, as shown in Figure 8.

Since the stress is given by equation (6.16), it should be kept in mind that the appearance of cracks is associated not only with the amplitude of the deformation but also with the total compressive load, P , *i.e.*, it will depend on the rate of deformation. If the load is much smaller than assumed here, the folding will take longer and cracks may not appear at all, or they may appear only at a much later stage when the folds are practically collapsed. (White, 1982)

We have assumed that the layers are of identical thickness and property, but this is not required, as shown hereafter. Consider a number of layers of thickness h_i and viscosity η_i . The compression acting in each of these layers is P_i , and the total thickness of the stack is H . The total transverse load, q , produced by the superposed layers is obtained by adding these loads for each layer. In other words, equation (4.10) for the single layer is replaced by

$$4\eta_1 l \frac{dw}{dt} = l^2 w \sum P_i h_i - \frac{1}{3} l^4 \frac{dw}{dt} \sum \eta_i h_i^3, \quad (7.3)$$

If we introduce the quantities

$$h = \sqrt{\frac{\sum \eta_i h_i^3}{\sum \eta_i h_i}},$$

$$\eta = \frac{\sum \eta_i h_i}{H}, \quad (7.4)$$

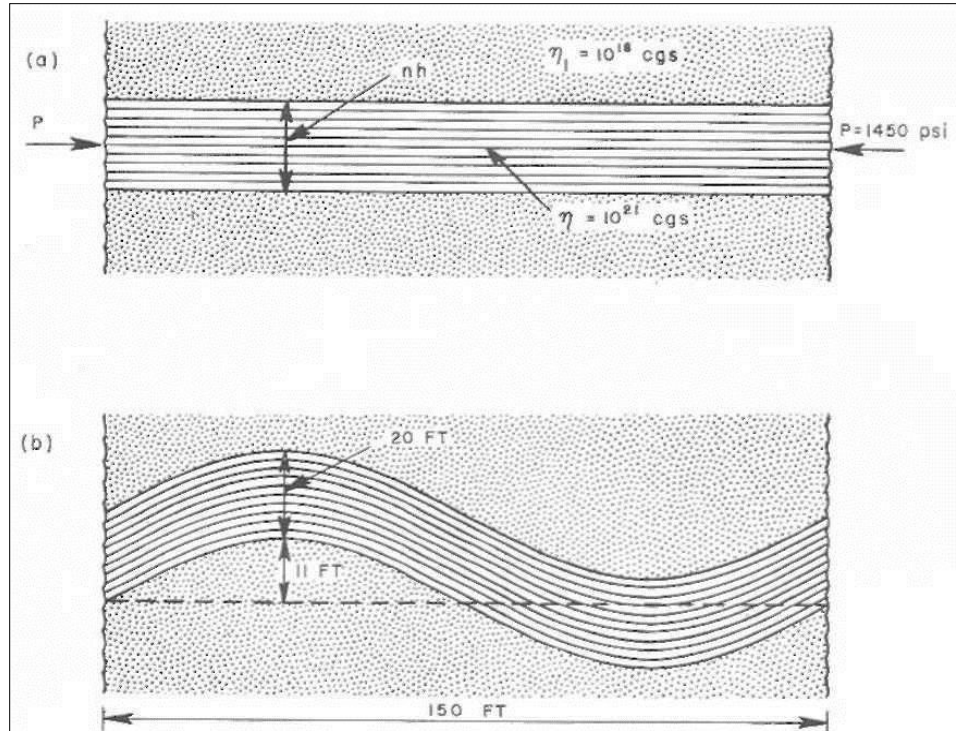


Figure 7 . Folding of a composite layer, (a) layer made of the superposition of 10 individual layers with a total thickness of 20 feet. Viscosities and compressive stresses the same as in Figure 6 . (b) Aspect of the folding after 15,500 years, assuming an initial deflection of one-quarter of an inch.

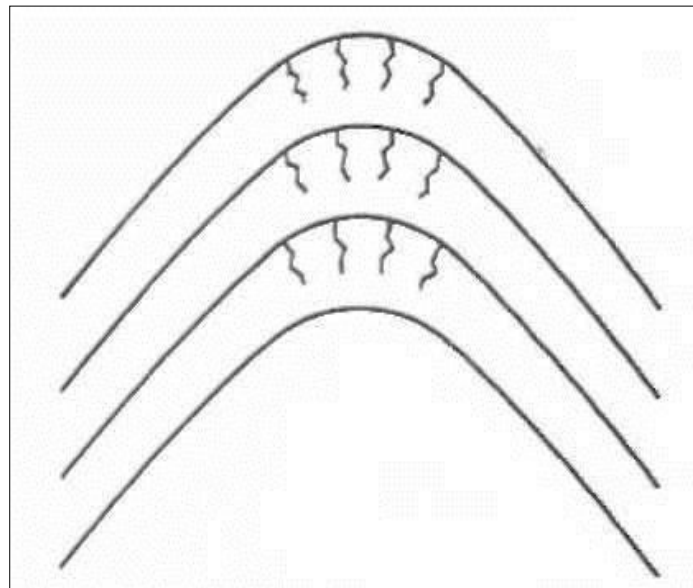


Figure 8 . sharpening of bends due to local yielding in the later phase of folding of the multiple-layered system of Figure 7 .

$$P = \sum \frac{P_i h_i}{h},$$

$$n = \frac{H}{h},$$

Equation (7.3) reduces to

$$\frac{4\eta_1}{n} l \frac{dw}{dt} = Phl^2w - \frac{1}{3} \eta h^3 l^4 \frac{dw}{dt}, \quad (7.5)$$

This is the same as the equation of folding for a *single* layer that has a thickness h , a viscosity η , is subject to a load P , and is surrounded by a medium of viscosity η_1/η . The rate of compressive strain of this fictitious layer under the load P is also the same as the actual system. A heterogeneous layered system of this type can, therefore, be analyzed by the methods exemplified heretofore. Once the over-all deformation has been determined, the bending stresses must be individually evaluated for each particular layer. The stress can easily be evaluated by calculating the bending moment in each layer, as is done for the case of the single layer.

It should be kept in mind that the present treatment of folding of multiple layers is approximate. (Cosgrove, 1976) We have assumed that the layer thickness remains constant. This, of course, is not the case. Because the normal loads in the layer add up, there is a limit in the present theory to the number of layers that can be stacked.

To complete this analysis, we shall also briefly mention the case of superposed elastic layers. By the same reasoning as before, examination of equation (3.14) leads to the conclusion that η superposed layers behave as a single one in a medium of viscosity η_1/η . Since the dominant wavelength for the elastic layer is independent of the viscosity, it has the same value (equation 3.18) as for the single layer. The rate of deformation is increased, however, but this does not change the comparison of the elastic case with the viscous case, as illustrated by the time scales of Tables 4 and 5, because both *cases* are affected by the same factor.

Although the assumption of perfect slip between layers will not be justified in general; one should keep in mind that, in many cases, layers of rock of low viscosity will alternate with layers of much higher viscosity. The latter will play the role of the actual layers considered in the theory, whereas the low-viscosity rock will behave more or less as an interfacial lubricant. We should also keep in mind the possibility of interfacial lubrication by the mechanism of hydraulic lifting in fluid-filled porous rock, as suggested by Hubbert and Rubey (1959) and (Drury, 1972) for over thrust faulting. The present analysis of the folding of multiple layers is a simplified one intended as a preliminary attack on the problem. A more elaborate treatment of the problem, which does not assume perfect interfacial slip, has been in preparation and will be presented at a later date.

It should be noted that if friction occurs between layers, the value for the dominant wavelength lies between that of a single solid layer of thickness $H = \eta h$ and that given by equation (7.1). The adherence will tend to increase the dominant wavelength somewhat above the latter value.

8. Influence of gravity on folding

In the geological scale the influence of gravity is of course a dominant factor. Its importance will vary, depending on the size of the folds, the density differences of the rock, and the proximity to the surface. We have limited ourselves to an analysis of the influence of gravity for two simple cases.

In one case, the layer lies on top of an infinitely deep medium. In the other, the layer lies between two infinite media of different densities. These two cases are closely related, and results from the first can be derived for the other. . A brief account of the results and elaboration on some applications follows.

Consider the case of a layer of viscosity η lying on top of an infinitely deep medium of viscosity η_1 and density ρ_1 (Figure 9).

Equation (4.10) for the deflection, w , of the layer is replaced by

$$Phl^2w - \frac{1}{3}\eta h^3 l^4 \frac{dw}{dt} = 2\eta_1 \frac{dw}{dt} + \rho g w, \quad (8.1)$$

If we compare this equation with equation (4.10), we notice that there is an additional term $p_1.gw$. This term introduces the effect of gravity and represents a "weight addition," positive or negative, associated with the rise or fall of the surface as it folds. Another difference is the replacement of the factor 4 by half its value. The latter change is due to the fact that the infinite medium lies only on one side of the layer, so that the lateral restraint to folding is reduced by half.

In the absence of gravity, the dominant wavelength for this case is given by

$$L_d = 2\pi h \sqrt[3]{\frac{\eta}{3\eta_1}}, \quad (8.2)$$

Comparing this with expression (4.13), we notice that the factor 6 is replaced by 3. This is again a consequence of the fact that the layer is restrained only on one side. . Let us assume a certain viscosity ratio, say, $\eta/\eta_1 = 500$. The ratio of the dominant wavelength of the layer to its thickness (L_d/h) is then a function only of the parameter $p/\rho_1 gh$ which embodies the influence of gravity. The value of (L_d/h) is shown in Figure 10 as a function of $\sqrt{p/\rho_1 gh}$. The square root of the parameter is represented along the abscissa because this yields a more convenient graph. Similar curves are also plotted for three other values of the viscosity ratio, η/η_1 .

We see from these results that gravity makes the dominant wavelength dependent on the load. A particular case of interest is that of a layer lying on a substratum whose viscosity is very small relative to that of the medium, *i.e.*, $\eta/\eta_1 = 0$. The dominant wavelength for this case is

$$L_d = 2\pi h \sqrt{\frac{2P}{\rho_1 gh}}, \quad (8.3)$$

This equation is represented by the limiting straight line in Figure 10 ($\eta_1 = 0$). We also note that there is no theoretical lower limit for the compression, P . Folding will occur no matter how low the compression. This is in contrast with the case of a purely elastic layer lying on a heavy fluid, discussed by Smoluchowski (1909a; 1909b; 1910) and Goldstein (1926), and shows the existence of a lower limit for P below which no instability appears. However, although there is no theoretical lower limit for P in the case of a viscous layer, there is a practical one which brings into consideration the rate of folding. Below a certain value of $p/\rho_1 gh$, the writer has shown that the amplification of the folding becomes insignificant. This region may be defined approximately by and corresponds to the left side of the shaded line in Figure 10.

$$\frac{P}{\rho_1 gh} \sim 9. \quad (8.4)$$

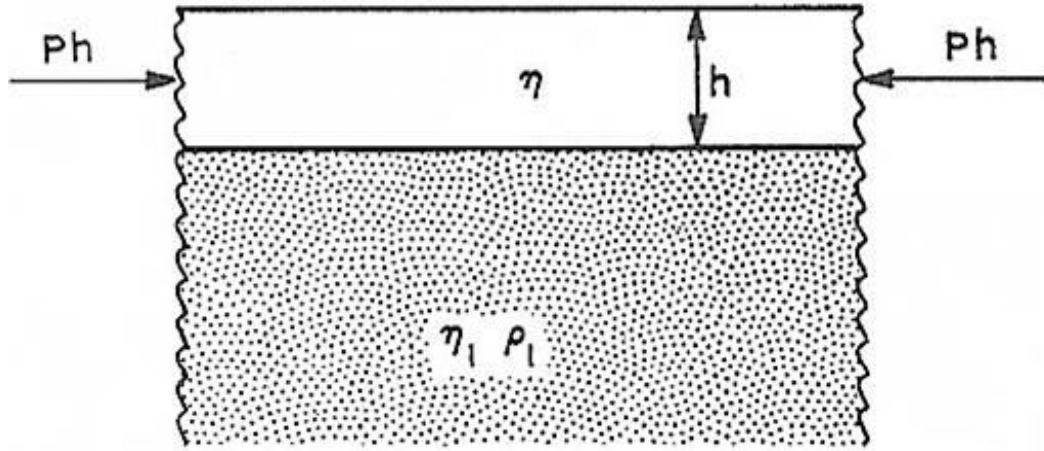


Figure 9 . Single layer of viscosity η on top of soft substratum of viscosity η_1 and density ρ_1 under a compressive stress P

This fact leads to an interesting conclusion. Suppose that we apply the highest possible load, *i.e.*, let it be of the order of the crushing strength $P = 14500 \text{ psi}$ ($P = 10^9 \text{ dynes/cm}^2$). If the thickness of the layer is such that the inequality (8.4) is satisfied,

$$h > \frac{P}{9\rho_1 g}, \quad (8.5)$$

For a density $\rho_1 = 2.5$ of the underlying material, this becomes

$$h \gtrsim 1500 \text{ feet}, \quad (8.6)$$

We have hence, for a thickness larger than 1500 *feet*, no significant folding will occur. With a lower value for P , say, 1450 *psi*, this limiting thickness would be reduced to 150 *feet*. As pointed out hereafter, this conclusion must be modified if we introduce the influence of surface erosion.

Another interesting conclusion can be drawn if we consider the wavelength. If we assume again that the compressive load is of the order of 14,500 *psi*, the longest possible wavelength corresponds to a thickness of 1500 *feet*. As shown by Figure 10, the wavelength at this limiting point is fairly independent of the viscosity ratio and is of the order of about 10 times the thickness, *i.e.*, $L_d = 15,000 \text{ feet}$. Wavelengths that is much larger than this will not occur in a single surface layer by the present mechanism of purely viscous folding.

We should point out that the analysis neglects the important factor of surface erosion. The effect of erosion is to remove matter from the crests while the troughs are filled by deposits. As indicated by Gunn (1937), the effect is approximately equivalent to a decrease in density. Hence, previous results can be used if we replace ρ_1 by an effective density $a\rho_1$, with $a < 1$. From Figure 10, we can see that this will generally increase the instability and the dominant wavelengths. Hence, if erosion is taken into account, wavelengths considerably larger than 15,000-20,000 feet are possible. Estimation of how large these can actually be in the earth on the basis of viscous folding requires the development of a more elaborate theory.

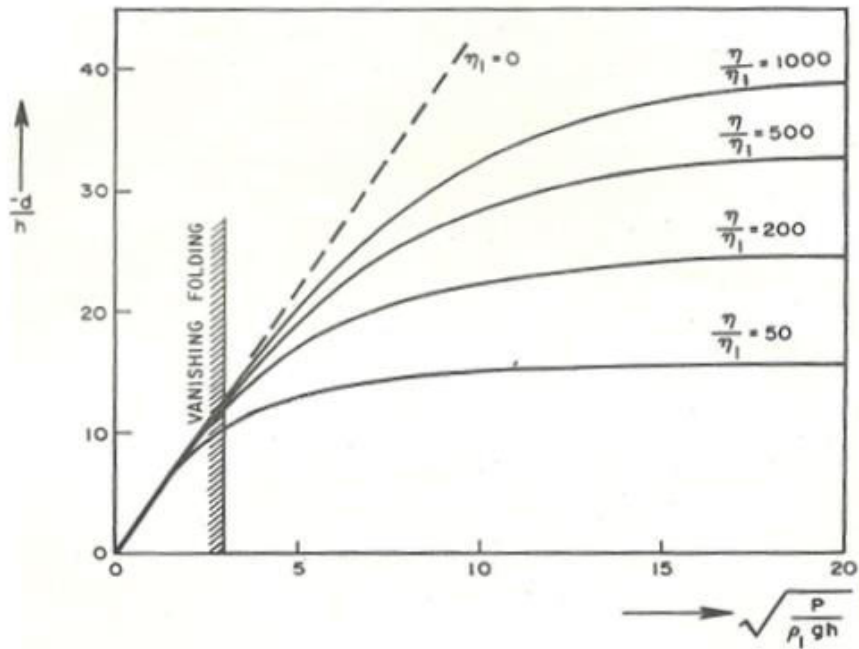


Figure 10 . Dominant wavelength, L_d plotted as the ratio L_d/h for the surface layer of Figure 9, when the combined effect of compressive stress P , gravity g , and viscosity ratio, η/η_1 , is taken into account

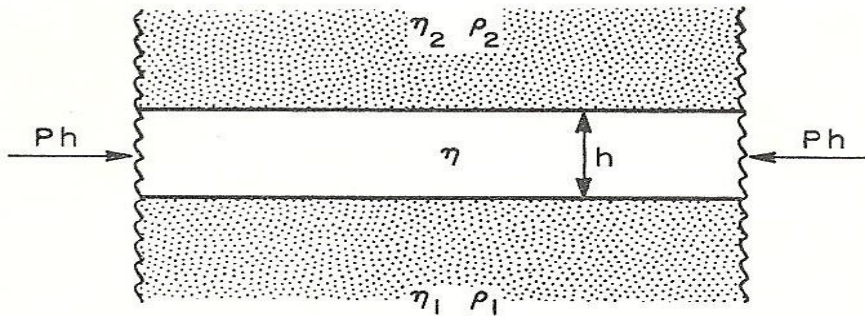


Figure 11. Layer embedded between two media of different viscosities and densities

The size of possible wavelengths is also increased if we consider the folding of multiple layers, as discussed hereafter.

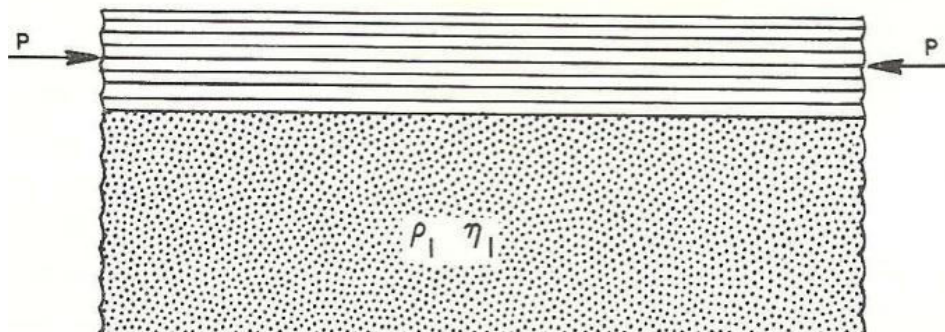


Figure 12 . Multiple superposed layers lying at the surface of a medium subject to gravity

In a more qualitative way, the mechanism of viscous folding in a gravity field can be explained as follows. A decrease in compressive load, P , or an increase in thickness will produce the same effect. Both cases correspond to a relative increase of the influence of gravity. The results just discussed lead to the conclusion that for a decrease in load below a certain value, which depends on the layer thickness, the effect of gravity takes over completely. The mechanism involved here is one of balance between the forces due to the compressive load, which produce the folding tendency, and the stabilizing influence of the gravity force, whose action tends to flatten out the folds. It is clear that in the absence of compression, a layer that is initially folded in a wavy surface will gradually be evened out and will approach a flat surface under its own weight. This last effect becomes predominant for the smaller values of the parameter p/ρ_1gh and the magnitude of the folding becomes insignificant compared to the over-all viscous shortening of the layer under the compression, P , which occurs during the same time.

The writer has discussed (1959 c) the case of a layer sandwiched between two infinite media of different densities in detail. Let us denote by p_1 and η_1 the density and viscosity of the bottom medium and by ρ_2 and η_2 the corresponding quantities for the top medium (Figure 11). We must distinguish two cases. In one, the bottom medium is heavier, i.e.,

$$\rho_1 > \rho_2. \quad (8.7)$$

In this case, the effect of gravity is stabilizing, and we can readily treat the problem by using the above results. We can repeat the same discussion used for the layer lying on top of the infinite medium and simply replace η_1 by $\eta_1 + \eta_2$ and p_1 by $\rho_1 - \rho_2$. When the top medium is the heavier, i.e.,

$$\rho_2 > \rho_1. \quad (8.8)$$

the effect of gravity is destabilizing, and spontaneous folding may occur without the compressive load.(Allison, 1979).

Of interest also is the influence of gravity in the case of a multiplicity of superposed layers; this was considered previously in this paper without gravity. Assume that we have such a system of superposed layers lying on top of an infinite medium of density p_1 and viscosity η_1 (Figure 12).

Let us proceed as in the derivation of equation (7.5). We shall use the same definitions for the factor η and the average quantities η , h and P expressed by equations (7.4). When all layers have the same thickness, h represents the thickness of each layer and n the number of layers. We apply the same reasoning as used in the derivation of equation (7.5), except that we now start from equation (8.1), which includes the effect of gravity. For multiple layers, this equation becomes

$$Phl^2w - \frac{1}{3} \eta h^3 l^4 \frac{dw}{dt} = \frac{2\eta_1}{n} \frac{dw}{dt} + \frac{p_1gw}{n}, \quad (8.9)$$

Comparison with equation (8.1) shows that the result is the same as that for the single layer of thickness h , except that the viscosity of the Bottom medium and the gravity, g , are both divided by n . We can therefore repeat exactly the same analysis, using the diagram of Figure 10 for the single layer. We can see that the effect of stacking layers is to increase the dominant wavelength proportionally to $\sqrt[3]{n}$ for cases where viscosity predominates and proportionally to \sqrt{n} for cases where gravity predominates.

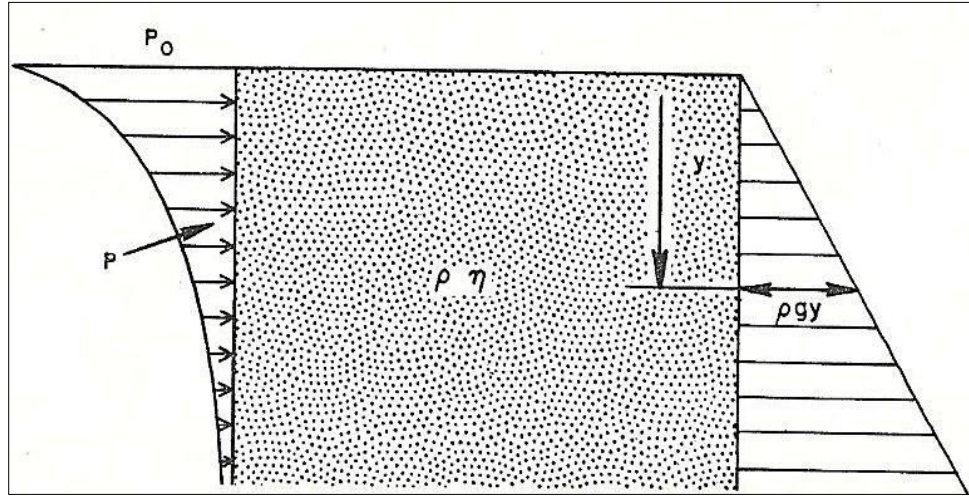


Figure 13 . Inhomogeneous viscous solid with a viscosity decreasing exponentially with the depth y . The initial stress is the hydrostatic pressure, pgy and a horizontal compression, P function of depth.

We must also replace g by g/n in the inequality (8.4). Correspondingly, the higher limit for the wavelength of viscous folding becomes of the order of 15,000 *n feet*. By the same reasoning used for the case of a single layer, we can see that the effect of erosion will increase. This will increase the higher limit even more. Regarding the assumption of perfect slip between layers, we refer to our remark at the end of Section 7 on the action of layers of low-viscosity rock and the mechanism of hydraulic lifting in fluid-filled porous rock suggested by Rubey and Hubbert (1959). (Cheeney, 1971) It can therefore be concluded that the large-scale folding associated with orogenesis is not incompatible with the mechanism of purely viscous folding of multiple layers.

As a matter of general interest, the problem of folding of an inhomogeneous but continuous solid (Figure 13) was also analyzed. In particular, we have considered a purely viscous and incompressible solid that is infinitely deep and such that its viscosity coefficient decreases exponentially with depth,

$$\eta = \eta_0 e^{-ry}, \quad (8.10)$$

This means that as we go deeper, the solid approaches the liquid state in a continuous manner. Originally, the material is in equilibrium under gravity, with a hydrostatic pressure, pgy proportional to the depth. We then assume that it is compressed horizontally at a uniform rate. This superimposes a horizontal compressive stress, P , which has a value of P_0 at the surface and which also decreases exponentially with depth:

$$P = P_0 e^{-ry}, \quad (8.11)$$

Under these conditions, the surface is found to be unstable, and folding will develop. The dominant wavelength of these folds is a function of a characteristic nondimensional parameter

$$G = \frac{\rho g}{P_0 r}, \quad (8.12)$$

(ρ is the mass density of the solid, and g is the acceleration of gravity) The dominant wavelength can be expressed as

$$L_d = \frac{2\pi}{r\delta}, \quad (8.13)$$

The non-dimensional quantity δ is a function of G , which has been determined numerically. The dependence of G on δ can be approximated by

$$\delta = 2.2G^{6/10}, \quad (8.14)$$

We conclude from this result that the presence of gravity is required in order for folding to occur. This can be seen by putting $g = 0$. In this case, the dominant wavelength, L_d , becomes infinite, and the folding disappears. This last conclusion depends, of course, on the assumption that the material is of infinite extent in the horizontal direction. If the surface extends over a distance D and is restrained at the ends, the wavelength will be determined by equation (8.13) if $L_d < D$. For larger wavelengths, or in the absence of gravity, the wavelength will be determined by the geometry of the constraint, and the surface will tend to bend in one-half wave of length D . The writer has discussed a numerical application of this result to examine the possibility of folding in the earth's crust as a whole by a purely viscous mechanism, based on a viscosity coefficient decreasing exponentially with depth (Biot, 1960). I assume that this constitutes an approximation for the viscosity of rock due to the increase of temperature and pressure with depth. For significant folding to occur, the viscosity must decrease by a factor smaller than $1/e$ in a depth of about 200 *feet* and the wavelength must not exceed 6000 *feet*. Such a viscosity gradient is considerably steeper than occurs on the average in the earth. Hence this model is not adequate to explain large-scale folding.

9 . Concluding remarks

The purpose of this paper has been to present a simplified and intuitive treatment of the theory of folding of stratified viscoelastic media along with Pachmarhis examples that are relevant in a geologic framework. The writer realizes that the geologic implications of the theory deserve a more elaborate discussion than has been given here. However, such a task lies beyond his particular field of competence.

In its present state the theory represents the first phase of a program. Its extension to materials and configurations of a more complex nature has been under development and will be presented at a later date.

It is difficult to assign specific values to the viscosity coefficients of rock except within one order of magnitude. Laboratory tests are restricted to time intervals that are extremely short in comparison with the geological time scale. On the other hand, a few observations have been reported of deformations occurring under natural conditions and known gravity forces over periods of the order of a century. Viscosities derived from such data agree in order of magnitude with the results from laboratory tests. The range of values, 10^{17} — 10^{22} poises, considered herein is probably on the high side if we take into account the fact that the viscosity drops quite rapidly with increasing pressure and temperature. Hence, the time required for folding at appreciable depth may be even smaller on the average than the figures given herein. Another feature involved here lies in the nature of the "effective viscosity coefficient" that must be introduced in the present theory when applied to materials of nonlinear properties as, for instance, when deformation rates increase faster than proportionally to the stress. As regards the viscosity contrast,

values of 100 to 1000 for the ratio of the viscosity of the layer to that of the embedding medium may be reasonably assumed as a representative order of magnitude for materials such as limestone or sandstone embedded in shale.

Within a lower stress range rocks are elastic for fast deformation and tend to behave approximately like a viscous medium for slow deformations. Results of the theory indicate that the viscous behavior predominates in tectonic folding. This leads to large deformations without fracture, and the dependence of fracture on deformation rates. This paper gives the time histories and rate processes and evaluates them numerically.

If one assumes that rocks behave as a purely viscous solid, significant folding may appear under relatively low tectonic stresses. However, in such a case the influence of gravity becomes important near the surface and may be sufficient to prevent folding. Even deep folds may be blocked by the presence of a stabilizing density gradient.

The theory is developed in the context of linear phenomena but is applicable to materials with nonlinear stress-strain relations. The linear theory may be looked upon as describing incipient folding in a state of initial plastic stress. The rheological behaviour in this case may be described by an "effective viscosity coefficient". In any case the incipient folding that is governed by the linear theory determines a wave length that is "frozen-in". As the folding proceeds, high stresses are produced at the crests. Cracks or accelerated creep are generated at these points, thus introducing another nonlinear feature. Owing to weakening at the bends, the bends tend to behave like hinges, and the folding then proceeds by a different mechanism that brings the crests closer together. The writer has also discussed another nonlinear feature of purely geometric origin by which folding tends to become more regular than predicted by the linear theory. This is due to the geometric limitation on folding beyond a certain amplitude: the waves of small amplitudes continue to grow at an exponential rate. In the light of the present remarks it should be remembered that wavelength predictions from the linear theory apply only to incipient folding. Therefore, any application to field observations when the folds are sharp requires an evaluation of the incipient configuration through an "unfolding process".

The time required for significant folding to occur has been evaluated. This evaluation is based on a range of acceptable tectonic stresses and rock viscosities. The results are in excellent agreement with the geological time scale based on radioactivity data. The geometric patterns of the folding derived from the present theory show a striking similarity to observed geological structures. This seems partly a consequence of two fundamental results of the theory. It was shown that for purely viscous deformations and when the influence of gravity is not important the dominant wave length is independent of the tectonic stress. This will, of course, remain approximately true for the case where viscous deformations play the important part. The other theoretical result involved here is the dependence of the dominant wave length on the cubic root of the viscosity ratio with the consequence that it is not sensitive to large variations in viscosity contrast.

Large-scale folding is compatible with the present theory, and the writer has shown that distances of a few between crests are possible by viscous deformation under the combined action of a horizontal compression and gravity. This conclusion, however, is not applicable if the crust is assumed to be of isotropic properties with a viscosity *d kilometers* increasing continuously with depth and a gradient corresponding to average properties in the earth. This is consistent with the usual assumption that stratification and discontinuities play an essential part in orogenic folding.

References

- Allison I, (1979). Variations of strain and microstructure in folded Pipe Rock in the Moine Thrust Zone at Loch Eriboll and their bearing on the deformational history Scottish Journal of Geology, ; 15(4): 263 - 269.
- Bijlaard, P. P., 1939, Het plooiën van een vlakke plaat die op een elastisch-isotrope half-ruimte is Opgelegd: De Ingenieur in Ned. Indie., no. 9, p. 215-226
- Bijlaard, P. P., 1947, On the elastic stability of thin plates supported by a continuous medium: Koninkl. Nederlandse, Akad. Wetensch. Proc, v. L, nos. 1 and 2, p. 79-193
- Biot, M. A., 1934, Sur la stabilité de l'équilibre élastique, équations de l'élasticité d'un milieu soumis à une tension initiale: Ann. Soc. Sci. de Bruxelles, tome 54, ser. B, pt. 1, p. 18-21
- Biot, M. A., 1938, Theory of elasticity with large displacements and rotations: 5th Internat. Cong. Applied Mechanics Proc, p. 117-122
- Biot, M. A., 1939, Théorie de l'élasticité du second ordre avec application à la théorie du flambage: Ann. Soc. Sci. de Bruxelles, tome 59, ser. 1, p. 104-112
- Biot, M. A. 1939, Non-linear theory of elasticity and the linearized case for a body under initial stress: Philos. Mag., v. 27, sec. 7, p. 468-489
- Biot, M. A. 1940, Elastizitätstheorie Zweiter Ordnung mit Anwendungen: Zeitschr. angew. Math, und Mech., bd. 20, no. 2, p. 89-99
- Biot, M. A. 1954, Theory of stress-strain relations in anisotropic viscoelasticity and relaxation phenomena: Jour. Applied Physics, v. 25, no. 11, p. 1385-1391
- Biot, M. A. 1956, Variational and Lagrangian methods in viscoelasticity: Berlin, Springer-Verlag, IUTAM Proc, Colloquium on deformation and flow of solids (Madrid, 1955), p. 251-263
- Biot, M. A. 1957, Folding instability of a layered viscoelastic medium under compression: Royal Soc. London *Proc.*, ser. A, v. 242, p. 444-454
- Biot, M. A. 1958, Linear thermodynamics and the mechanics of solids: 3d U.S. Natl. Cong. Applied Mechanics, American Soc. Mechanical Engineers Proc, p. 1-18
- Biot, M. A. 1958, Stability problems of inhomogeneous viscoelastic media: New York, Pergamon Press, IUTAM Proc, Colloquium on inhomogeneity in elasticity and plasticity (Warsaw, September 1958), p. 311-321
- Biot, M. A., 1959, Folding of a layered viscoelastic medium derived from an exact stability theory of a continuum under initial stress: Applied Mathematics Quart., v. XVII, no. 2, p. 185-204
- Biot, M. A., 1959b, On the instability and folding deformation of a layered viscoelastic medium in compression: Jour. Applied Mechanics, ser. E, v. 26, p. 393-400
- Biot, M. A., 1959, The influence of gravity on the folding of a layered viscoelastic medium under compression Jour. Franklin Inst., v. 267, no. 3, p. 211-228-- 1960, Instability of a continuously inhomogeneous viscoelastic half-space under initial stress: Jour. Franklin Inst., v. 270, no. 3, p. 190-201
- Biot, M. A., Ode, H., and Roever, W. L., 1961, Experimental verification of the theory of folding of stratified viscoelastic media: Geol. Soc. America Bull., v. 72, p. 1621-1632
- Birch, Francis, Schairer, J. F., and Spicer, H. Cecil, 1942, Handbook of physical constants: Geol. Soc. America Special Paper 36, 325 p.
- Burg J.-P. and Podladchikov Y. (1999) From buckling to asymmetric folding of the continental lithosphere: numerical modelling and application to the Himalayan syntaxes Geological Society, London, Special Publications, 2000; 170(1): 219 - 236. Fernandez C. and Castro A. Brittle behaviour of granitic magma: the example of Puente del Congosto, Iberian Massif, Spain Geological Society, London, Special Publications, ; 168(1): 191 - 206.
- Butler R. W. H., Spencer S., and Griffiths H. M. (1998) The structural response to evolving plate kinematics during ranspression: evolution of the Lebanese restraining bend of the Dead Sea Transform Geological Society, London, Special Publications, ; 135(1): 81 - 106.
- Burg J.P. and Ford M. (1997) Orogeny through time: an overview Geological Society, London, Special Publications, 121(1): 1 - 17.
- Cosgrove J. W. (2007) The use of shear zones and related structures as kinematic indicators: a review Geological Society, London, Special Publications,
- Camerlo R. H. and Benson E. F. Geometric and seismic interpretation of the Perdido fold belt: North western deep-water Gulf of Mexico AAPG Bulletin,; 90(3): 363 - 386.
- Cosgrove j. W. (2006) the formation of crenulation cleavage Journal of the Geological Society, ; 132(2):

155 - 178.

- Cheeny R. F. (1971) Strain-rates, folding and cleavage *Scottish Journal of Geology*,; 7(4): 345 - 348.
- Drury S. A. (1972) The tectonic evolution of a Lewisian complex on Coll, Inner Hebrides *Scottish Journal of Geology*,; 8(4): 309 - 333.
- Ferrill D. A. and Morris A. P. (2008) Fault zone deformation controlled by carbonate mechanical stratigraphy, Balcones fault system, Texas AAPG Bulletin, ; 92(3): 359 - 380.
- Goguel, J., (1943), Introduction a Petude mecanique des deformations de Pecorce terrestre: Paris, Memoire, Ministere de la Production Industrielle et des Communications, Imprimerie Nationale, 514 p.
- Goldstein, S (1926), The stability of a strut under thrust when buckling is resisted by a force proportional to the displacement: *Cambridge Philos. Soc. Proc*, v. 23, p. 120-129
- Gough, G. S., Elam, C. F., and DeBruyne, N. A., (1940) , The stabilization of a thin sheet by a continuous supporting medium: *Jour. Royal Aeronautical Soc*, v. 44, p. 12-43
- Griggs, D. T., (1939), Creep of rocks: *Jour. Geology*, v. 47, p. 225-251 - 1940, Experimental flow of rocks under conditions favoring recrystallization: *Geol. Soc. America Bull*, v. 51, p. 1001-1022
- Gunn, Ross, (1937), A quantitative study of mountain building on an unsymmetrical earth: *Jour. Franklin Inst.*, v. 224, no. 1, p. 19-53
- Horsman E., Tikoff B. , and Czeck D. (2008) Rheological implications of heterogeneous deformation at multiple scales in the Late Cretaceous Sierra Nevada, California *Geological Society of America Bulletin*,; 120(1-2): 238
- Hickey K.A. and Bell T.H. (2001); Resolving complexities associated with the timing of macroscopic folds in Multiply deformed terrains: The Spring Hill synform, Vermont *Geological Society of America Bulletin*, 113(10): 1282
- Hutton D. H. W. (1982) A tectonic model for the emplacement of the Main Donegal Granite, NW Ireland *Journal of the Geological Society*,; 139(5): 615 - 631.
- Hide, R., (1955), The character of the equilibrium of an incompressible viscous fluid of variable density: an approximate theory* *Cambridge Philos. Soc Proc*, v. 51, pt. 1, p. 179-201
- Hubbert, M. King, and Rubey, William W., (1959), Mechanics of fluid-filled porous solids and its applications to overthrust faulting: *Geol. Soc. America Bull.*, v. 70, p. 115-166
- Kaisin, F., (1927), Deformation de Plaques de Marbre dans des Monuments Anciens de Bruges: *Ann. Soc Sci. de Bruxelles*, tome 47, ser. B, pt. 1, p. 192-194
- Kienow, S., (1942), *Grundziige einer Theorie der Faltungs- und SchieferungsvorgSnge*: Berlin, Borntr&ger, Fortschritte der Geologie und Paleontologie, bd. XIV, h. 46
- Kulp, J. Laurence, (1959), Absolute age determination of sedimentary rocks: 5th World Petroleum Cong., sect. 1, Paper 37, p. 689-704
- Passchier C. W. , Zhang J. S., and Konopasek J. (2005) Geometric aspects of synkinematic granite intrusion into a ductile shear zone -- an example from the Yunmengshan core complex, northern China *Geological Society, London, Special Publications*, 245(1): 65 - 80.
- Rubey, William W., and Hubbert, M. King, (1959) , Overthrust belt in geosynclinal area of western Wyoming in light of fluid-pressure hypothesis: *Geol. Soc America Bull.*, v. 70, p. 167-205
- Srivastava D. C. and Rastogi V. HingeInflex : (2010) a matlab-based method for precise selection of the hinge and the inflection points in folds *Geological Magazine*, ; 147(2): 233 - 241.
- Slim, A.C, Balmforth, N.J Craster R.V, and Miller J.C (2009) Surface wrinkling of a channelized flow *Proc R Soc A*,; 465(2101): 123 - 142.
- Simpson G. (2006) Influence of erosion and deposition on deformation in fold belts *Geological Society of America Special Papers*,; 398(0): 267 - 281.
- Scanlin M. A. and Engelder T. (2003); The basement versus the no-basement hypotheses for folding within the Appalachian plateau detachment sheet *Am J Sci*, 303(6): 519 - 563.
- Stipska P., Schulmann K., and Hock V (1999) Complex metamorphic zonation of the Thaya dome: result of buckling and gravitational collapse of an imbricated nappe sequence *Geological Society, London, --Special Publications*, ; 169(1): 197 - 211.
- Smoluchowski, M., (1909) Uber ein gewisses—Stabilitatsproblem der Elastizit&tslehre: *Akad. Wiss. Krakau. Math. KX*, p. 3-20
- Smoluchowski, M (1909) , Kilka Uwag o Fizycznych Podstawach Teoryi Gorotworczych (Einige

Bemerkungen über die physikalischen Grundlagen der Theorien der Gebirgsbildung): Kosmos, v. XXXIV, p. 547-579 (Annals of the Copernicus Society published by Gubrynowicz and Schmidt, Lwow)

Smoluchowski, M (1910), Versuche über Faltungserscheinungen schwimmender elastischer Platten: Akad. Wiss. Krakau. Math. KX, p. 727-734

Van der Neut, (1943), Die Stabilität geschichteter Streifen: Natl. Luchtvaart Laboratorium, Bericht S. 284

White R. S.(1982). Deformation of the Makran accretionary sediment prism in the Gulf of Oman (north-west Indian Ocean) Geological Society, London, Special Publications,; 10(1): 357 - 372.
